Late Pleistocene slip on a low-angle normal fault, Searles Valley, California

Tye Numelin
Eric Kirby
Department of Geosciences, The Pennsylvania State University, University Park, Pennsylvania 16802, USA

J. Douglas Walker
Brad Dideriksen
Department of Geology, University of Kansas, Lawrence, Kansas 66045, USA

ABSTRACT

The mechanical feasibility of normal-sense slip on low-angle faults remains a conundrum in extensional tectonics. The rarity of demonstrably active low-angle normal faults may imply that very specific criteria must be satisfied for significant fault displacement. We present new geologic observations, geomorphic mapping, and structural analysis for a low-angle fault zone along the eastern margin of Searles Valley, California. Our observations indicate that Pleistocene displacement along the range-front fault scarps is the near-surface expression of slip on a bedrock-rooted low-angle normal fault. Along the central portion of the range front in Searles Valley, high-angle faults offset late Pleistocene alluvial and lacustrine surfaces. These faults merge downward into a west-dipping, low-angle fault, but do not displace the low-angle surface. These geometric relations are satisfied only when displacement on the high-angle faults is accommodated by slip on the basal low-angle fault. We use displaced alluvial fan surfaces to determine slip rates across the fault system over late Pleistocene to Holocene time. Combining radiocarbon ages of lacustrine tufa deposits with high-precision topographic surveys of fault scarps yields average slip rates of 0.21–0.35 m/k.y. Additional mapping of faults within the Slate Range at the northern end of Searles Valley suggests that slip is transferred northward to the Manly Pass fault, a bedrock normal fault that trends northeast into Panamint Valley. Thus, although displacement along the range-front fault system dies out northward, we infer that active deformation occurs within the range and likely links extension in Searles Valley with deformation in Panamint Valley.

Keywords: Eastern California shear zone, low-angle normal fault, neotectonics, Searles Valley, Panamint Valley, California.

INTRODUCTION

The mechanical feasibility of normal-sense displacement on low-angle fault systems remains one of the outstanding challenges to understanding large-magnitude extension of the lithosphere. Despite overwhelming geologic evidence from both continental and oceanic realms indicating that low-angle normal faults are common, if not ubiquitous, features of extended crust (see reviews by Wernicke, 1995; Axen, 2004), debate remains regarding how such structures initiate and are maintained at low angles (e.g., Lavier and Buck, 2002). The persistence of this debate reflects, in part, the relative paucity of demonstrably active low-angle normal fault systems (Caskey et al., 1996; Axen et al., 1999; Boncio et al., 2000; Hayman et al., 2003). Seismicity on such fault systems is even more rare (Jackson and White, 1989; Abers et al., 1997; Abbott et al., 2001), and has been interpreted to reflect either long recurrence times between earthquakes or aseismic slip (Wernicke, 1995). Demonstration of active slip on low-angle fault systems, characterization of slip rates, and investigations of seismic behavior are thus critical steps toward a deeper understanding of these enigmatic structures.

Since the recognition of low-angle normal faults in the Basin and Range province of the western United States (Longwell, 1945), this region of highly extended lithosphere has motivated a broad body of work documenting Tertiary slip on these structures (cf. Axen, 2004). However, nearly all of these structures appear to be inactive today, and most extension in the upper crust is accommodated by relatively high angle normal faults (e.g., Friedrich et al., 2004). Notable exceptions occur in Dixie Valley, Nevada, where geologic and geophysical data indicate that a historic surface rupture occurred on a low-angle fault plane (Caskey et al., 1996; Abbott et al., 2001); in Baja California, where faults cutting Pliocene–Pleistocene deposits are compatible with slip on a low-angle detachment (Axen et al., 1999); and in the Death Valley region, where low-angle normal faults have been argued to remain active into Quaternary time (Burchfiel et al., 1987).

The geometry of faults in this latter region, however, remains the subject of some debate. The southwestern Basin and Range was subjected to large-magnitude crustal extension beginning in Miocene time (Wernicke and Snow, 1998); previous workers have estimated that >100 km of west-northwest–directed extension between the Sierra Nevada and the Spring Mountain blocks (Fig. 1) has been accommodated on regionally extensive low-angle normal fault systems (e.g., Niemi et al., 2001; Snow and Wernicke, 2000). Field observations of crosscutting relationships between high- and low-angle normal faults have led a number of workers to consider these low-angle systems to be inactive at present (Miller, 1999, Cichanski, 2000), abandoned in favor of high-angle fault systems kinematically linked to right-lateral strike-slip faults (Burchfiel and Stewart, 1966; Zhang et al., 1990; Miller, 1999; Cichanski, 2000). Moreover, regional magnetotelluric data image steeply dipping zones of high electrical conductivity that are correlated with the surface trace of active faults (Park and Wernicke, 2003).

Geosphere; Month 2007; v. 3; no. 3; p. 163–176; doi: 10.1130/GES00052.1; 11 figures; 3 tables.

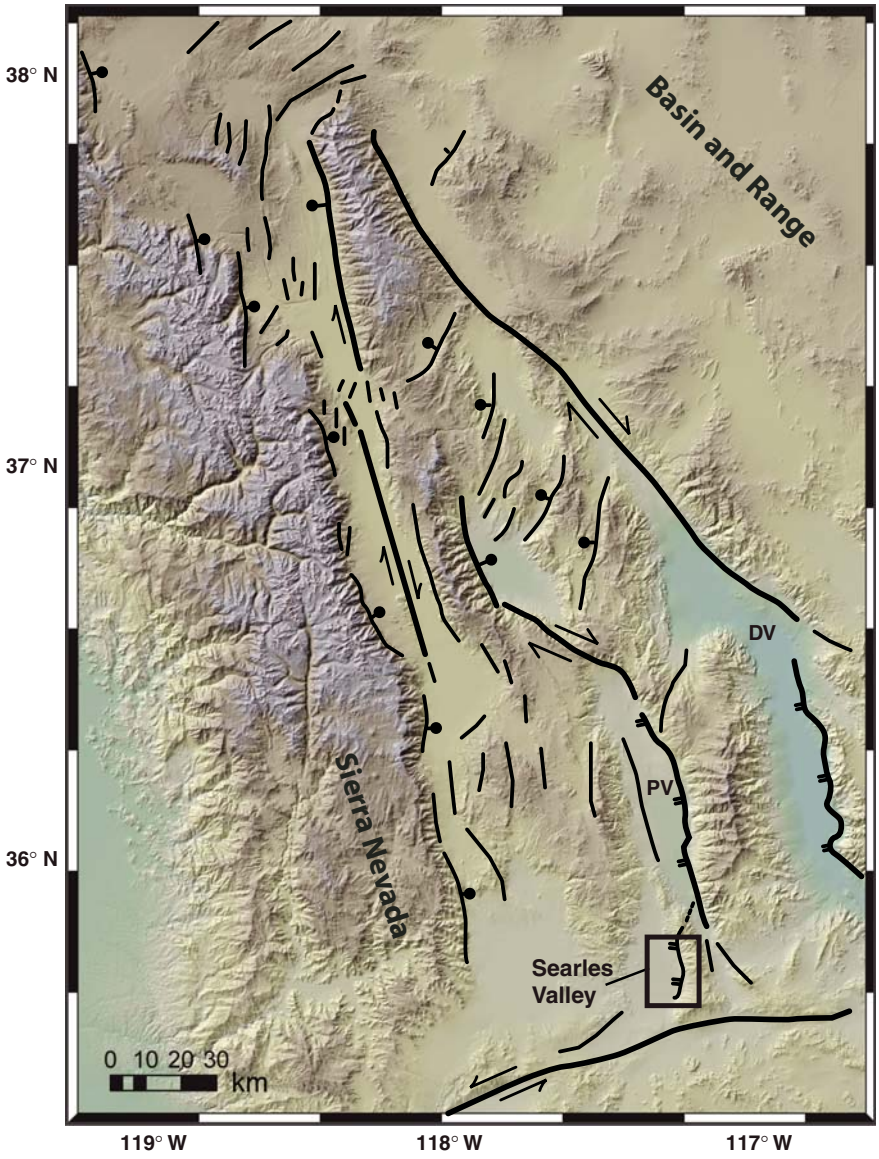

Figure 1. Color-shaded digital elevation map of southwestern Basin and Range and the Eastern California shear zone–Walker Lane. Major active fault systems are annotated. SV—Searles Valley; PV—Panamint Valley; DV—Death Valley.

In contrast, recent field studies of Quaternary deformation above the Black Mountain (Hayman et al., 2003) and Panamint Valley faults (Kirby et al., 2003) suggest that faults within alluvial deposits are kinematically compatible with extension above low-angle detachments.

In this paper we present geologic observations that indicate that late Pleistocene–Holocene normal faulting along the eastern margin of Searles Valley was associated with slip on a low-angle normal fault. Previously recognized low-angle structures within the Slate Range (Searles Valley fault; Walker et al., 2005) root down to the west, beneath Searles Valley (Fig. 1). Our mapping demonstrates that active faults along the base of the Slate Range (Tank Canyon fault zone; Smith et al., 1968; Wesnousky, 1986) are kinematically linked to slip on the Searles Valley fault. In contrast to most previous studies arguing for or against scarp-forming slip on detachment systems (e.g., Axen et al., 1999; Cichanski, 2000), exposures along the Searles Valley fault systems allow direct observation of the interaction between high-angle normal faults that displace late Pleistocene alluvial and lacustrine deposits and a rooted low-angle normal fault. Moreover, reconstruction of the magnitude of displacement from offset alluvial and lacustrine deposits allows us to place bounds on the slip rates along this fault during late Pleistocene and Holocene time.

GEOLOGIC SETTING

Active faulting within eastern California accommodates right-lateral transtension between the Sierra Nevada and the Basin and Range province (Dokka and Travis, 1990; Dixon et al., 2003; Unruh et al., 2003), a region that has come to be known as the Eastern California shear zone. Geodetic studies indicate that right-lateral shear accounts for ~20%–25% of the relative plate motion between the Pacific and North American plates (Dixon et al., 1995, 2000, 2003; Gan et al., 2000; Miller et al., 2001; Bennett et al., 2003). Regional palinspastic reconstructions suggest that the onset of right-lateral shear in this portion of the Basin and Range occurred during late Miocene or early Pliocene time (Wernicke and Snow, 1998; Snow and Wernicke, 2000; McQuarrie and Wernicke, 2005), perhaps coincident with a change in the relative motion between the Pacific and North American plates (Atwater and Stock, 1998).

The role of low-angle normal faults during Miocene–Holocene transtension in eastern California remains the subject of some debate. Although northern Panamint Valley (Fig. 2, inset) appears to have opened on a low-angle fault system (Burchfiel et al., 1987; MIT and Biehler, 1987), other workers have suggested that detachment faults have been abandoned in favor of a high-angle range-front fault system (Zhang et al., 1990; Miller, 1999; Cichanski, 2000) linked to steep strike-slip faults at depth (Park and Wernicke, 2003). In addition to debate over the significance of low-angle fault systems in this region, a persistent discrepancy exists between geodetic measures of velocity (Miller et al., 2001) and geologic slip rates (Zhang et al., 1990; Beanland and Clark, 1994; Reheis and Sawyer, 1997) across the Eastern California shear zone. Although recent interpretations have suggested that the surface velocity field is transient, reflecting variations in the seismic cycle (e.g., Peltzer et al., 2001; Dixon et al., 2003), this hypothesis remains difficult to test, due in large part to relatively poor characterization of slip rates on many of the major fault systems over late Pleistocene time.

Searles Valley is an ~450 km^2 teardrop-shaped valley located north of the Garlock fault in the southwestern Basin and Range. The valley is bound on the west by the Argus Range and on the east by the Slate Range (Fig. 2, inset). An ~20-km-long network of active normal faults, termed the Tank Canyon fault zone by Wesnousky (1986), is developed within alluvial deposits along the eastern edge of the valley. Wesnousky (1986) assigned a minimum slip rate of ~0.5 mm/yr and a maximum rate of ~1.6 mm/yr, with a preferred slip rate

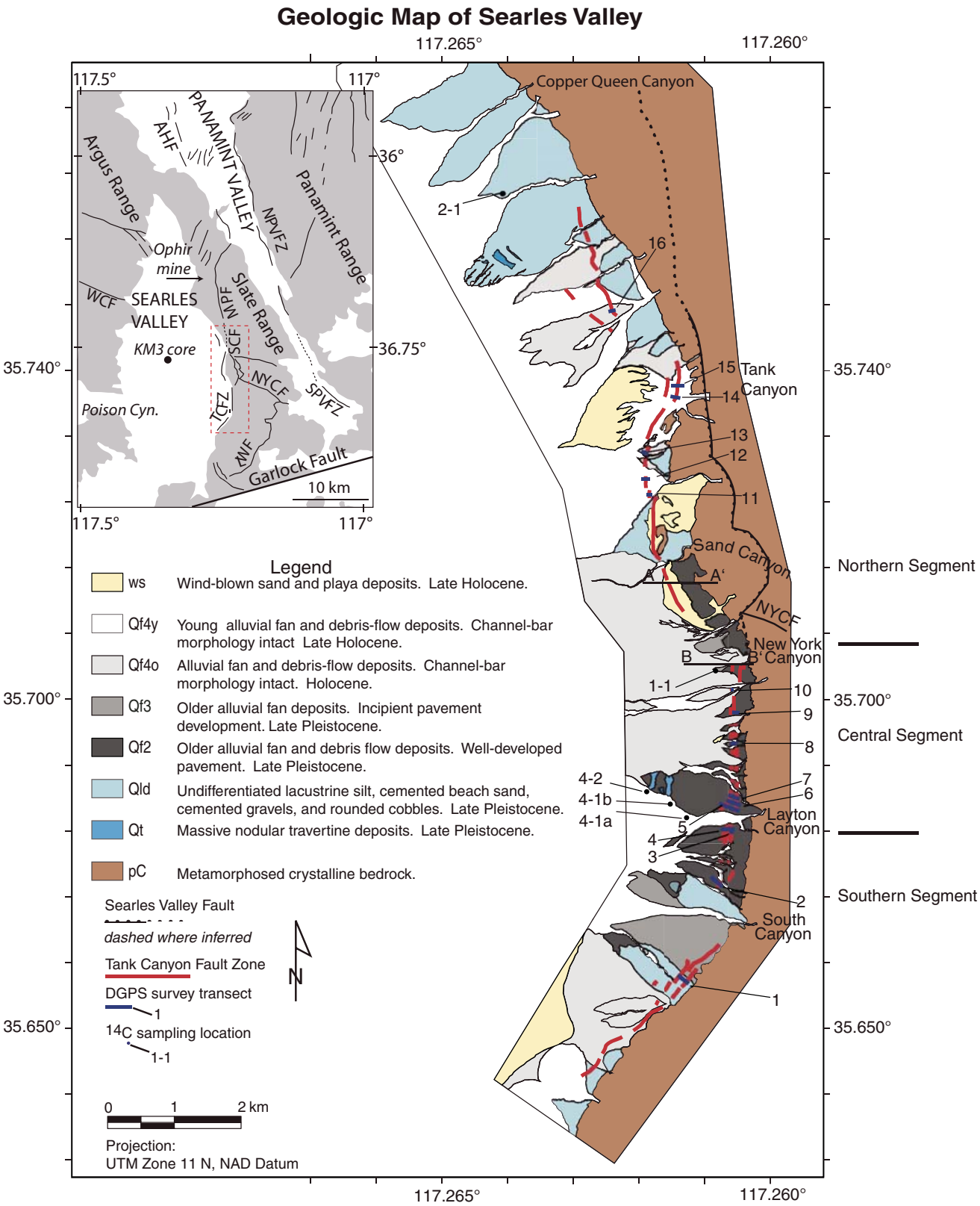

Figure 2. Geologic map of the western front of the Slate Range. The Differential Global Positioning Satellite (DGPS) topographic surveys across fault scarps are traced in blue and numbered (1–16). Solid black circles are sampling locations for ^{14}C, labeled according to Table 2. Inset shows tectonic setting of Searles Valley study area. Location of KM3 borehole is shown. Red box outlines the mapping area. Major faults: WCF—Wilson Canyon, AHF—Ash Hill, MPF—Manly Pass, SCF—Sand Canyon, TCFZ—Tank Canyon fault zone, NYCF—New York Canyon, LWF—Layton Well, NPVFZ—Northern Panamint Valley, SPVFZ— Southern Panamint Valley.

of 1.0 mm/yr to this fault system. These numbers, however, are largely based on a regional chronology developed by Smith et al. (1968), and no comprehensive study of the active fault system has been conducted. In this contribution, we develop an argument that the range-front fault system is linked to low-angle structures within the Slate Range, and consequently follow Walker et al. (2005) in referring to the entire fault array as the Searles Valley fault system.

The bedrock geology of the Slate Range, in contrast, is fairly well known, following the pioneering work of Smith et al. (1968); these workers interpreted several large west-northwest–dipping low-angle faults within the range as thrust faults, acknowledging that their displacement history was enigmatic. Recent mapping (Didericksen, 2005; Walker et al., 2005) shows that one of these, the Searles Valley fault (previously termed the Sand Canyon thrust; Smith et al., 1968), accommodated primarily normal displacement during Tertiary time. The Searles Valley fault trends northward within the Slate Range and connects to a west-dipping fault zone exposed in Manly Pass (Fig. 2, inset) (Walker et al., 2005). Although first mapped as a zone of complex shear fabrics developed in pre-Cenozoic rocks (Smith et al., 1968), the Manly Pass fault is marked by a moderately west dipping zone of fault gouge that separates deformed Tertiary volcanic rocks and Pliocene fanglomerates in the hanging wall from deformed crystalline rocks in the footwall (Walker et al., 2005; Didericksen, 2005). Subhorizontal faults that omit section are also recognized in the central Slate Range (Smith et al., 1968; Didericksen, 2005; Walker et al., 2005). These structures, thought to be Tertiary in age (Walker et al., 2005), are cut by the low-angle Searles Valley fault system (Didericksen, 2005), indicating that the Searles Valley fault represents the youngest structure within the range. Our study is motivated by the recognition that the southward projection of the Searles Valley fault is nearly coincident with the surface trace of active scarps along the range front south of Sand Canyon (Fig. 2). Thus, it is possible that scarps of the range-front fault system are simply the expression of recent slip along the Searles Valley fault system. We seek to test this hypothesis via geologic mapping and investigation of the geometry and kinematics of recent faulting along the range front.

STRATIGRAPHY OF LATE PLEISTOCENE ALLUVIAL DEPOSITS

Fault scarps along the eastern margin of Searles Valley displace a series of alluvial fan and lacustrine deposits that record fluctuations in the level of Searles Lake. Through much of the Quaternary, Searles Lake formed the terminus of a chain of pluvial lakes that drained the eastern margin of the Sierra Nevada (e.g., Jannik et al., 1991). Of interest to this study, however, are variations in lake level during the latest Pleistocene. Smith and Street-Perrott (1983) reconstructed lake-level histories (Fig. 3) spanning the period from 35 ka to present using surface outcrops near Poison Canyon (Fig. 2, inset) and core material from the center of the basin. Radiocarbon dating of lacustrine tufas and salts yielded evidence for a prolonged highstand from ca. 21 to 16 ka and a brief reoccupation of the highstand shoreline between ca. 12 and 10 ka (see discussion in McGill and Sieh, 1991). The lake appears to have been completely desiccated by ca. 10 ka (Smith and Street-Perrott, 1983). Lin et al. (1998) reevaluated this chronology using U-series dating of lacustrine tufas at Poison Canyon, and found that reservoir-corrected ^{14}C ages were consistently younger than U-series ages from the same samples; they attributed the discrepancy to contamination of outcrop tufa samples by modern carbon. Thus, the lake-level curve of Smith and Street-Perrott (1983) may underestimate the true ages by 1–2 k.y.

Surficial deposits exposed along the eastern margin of Searles Valley are either lacustrine sediments that accumulated in Searles Lake, or intercalated alluvial fans shed from the Slate Range to the east. Lacustrine deposits (Qld, Fig. 2) near the range front are typically clast-supported, subrounded gravels and well-sorted sands, which we interpret to represent beach and/or shoreline deposits at the former lake margin. Many of these exposures are associated with wave-cut platforms and cliffs. The most prominent of these shorelines is at an elevation of ~690 m, near the head of alluvial fans along the central part of the range. Beach facies grade into fine-grained units toward the center of the valley. These lacustrine deposits are primarily gray to green silts and muds that record deeper-water deposition (Smith et al., 1968). In addition, exposures of lacustrine deposits are commonly associated with thin to massive accumulations of buff-colored nodular travertine (Smith et al., 1968) (Qt in Fig. 2). In general, fan deposits are composed of coarse cobbles and boulders that range from subrounded to subangular. Deposits range from matrix to clast supported, and likely represent both sheetwash and/or flood deposits and debris flows. As a whole, these deposits are relatively thin (1–5 m) and overlie lacustrine units.

We distinguish the relative age of alluvial fan deposits based on both the surface morphology and degree of pavement development (Table 1). The younger fans (Qf4o and Qf4y) exhibit well-preserved depositional morphology (bar and swale) with little to no pavement development

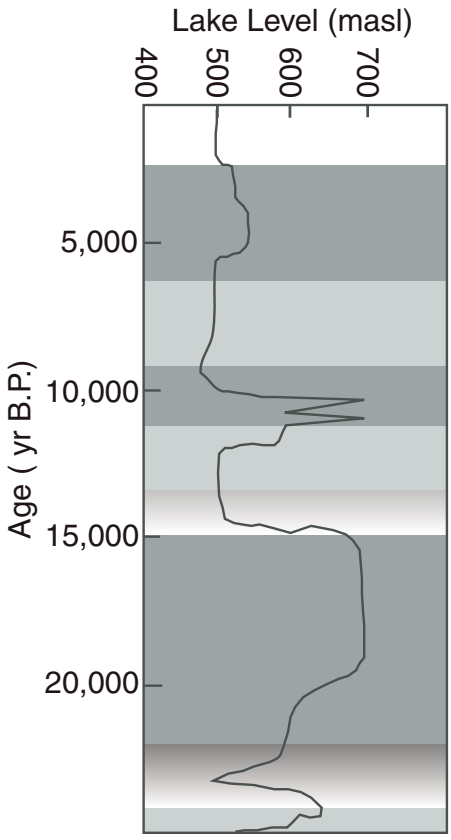

Figure 3. Lake-level history (masl—meters above sea level) for Searles Lake from 25 ka to present (Smith et al., 1983). Shaded areas represent chronostratigraphic intervals from Smith and Street-Perrott (1983). Gradients represent their uncertainty in the age cutoffs.

(Table 1). These fans are inset against older alluvial deposits (Qf2 and Qld) near the range front, and they broaden basinward to form coalesced aprons of alluvium (Fig. 2). Two older fan surfaces (Qf2, Qf3) are preserved slightly above (1–4 m) Qf4 surfaces; Qf3 deposits are inset against Qf2 deposits. Both sets of fan surfaces exhibit moderate pavement development characterized by clasts with a deep brown varnish coating and rubified undersides. These surface clasts overlie a thin (5–10 cm) vesicular (Av) soil horizon (Table 1).

These stratigraphic relationships between alluvial and lacustrine deposits within the central portion of Searles Valley are key to understanding the timing of recent slip along the range-front fault. Near the head of Layton Canyon (Fig. 2), well-sorted beach gravel is associated with a prominent wave-cut bench in bedrock 4–6 m in height (Fig. 4). This bench occurs at ~690 m elevation and is the highest shoreline developed continuously around the southeast valley margin. From the continuity of the shoreline and its

TABLE 1. DESCRIPTION OF MAP UNITS IN SEARLES VALLEY

Map symbol	Surface Form	Desert varnish	Soil development	Depositional environment
ws	Subtle dunes	None	None	Eolian
Qf4y	Channel levees; prominent bar and swale; no pavement	None	None	Alluvial fan/debris flow
Qf4o	Channel levees; prominent bar and swale; no pavement	Rare (clasts with varnish coating are likely erratics)	None	Alluvial fan/debris flow
Qf3	Dissected; no bar and swale; incipient pavement development: patchy flat areas with loosely interlocking subangular clasts	Discontinuous, deep-brown varnish	Av horizon: silty; 0–0.1 m thick B horizon: silt and clay; dense	Alluvial fan/debris flow
Qf2	Dissected; no bar and swale; incipient pavement development: patchy flat areas with tightly interlocking rounded to subrounded clasts	Continuous; shiny, deep-brown varnish	Av horizon: silty; 0–0.2 m thick B horizon: silt and clay; dense	Alluvial fan/debris flow
Qld	Dissected; preserved paleoshorelines; carbonate cemented subangular to rounded alluvial clasts with local grading to rounded beach gravels	None	Rare pedogenic hardgrounds	Near-shore lacustrine/ beach
Qt	Dissected convex tufa and travertine mounds	None	NA	Shallow lacustrine

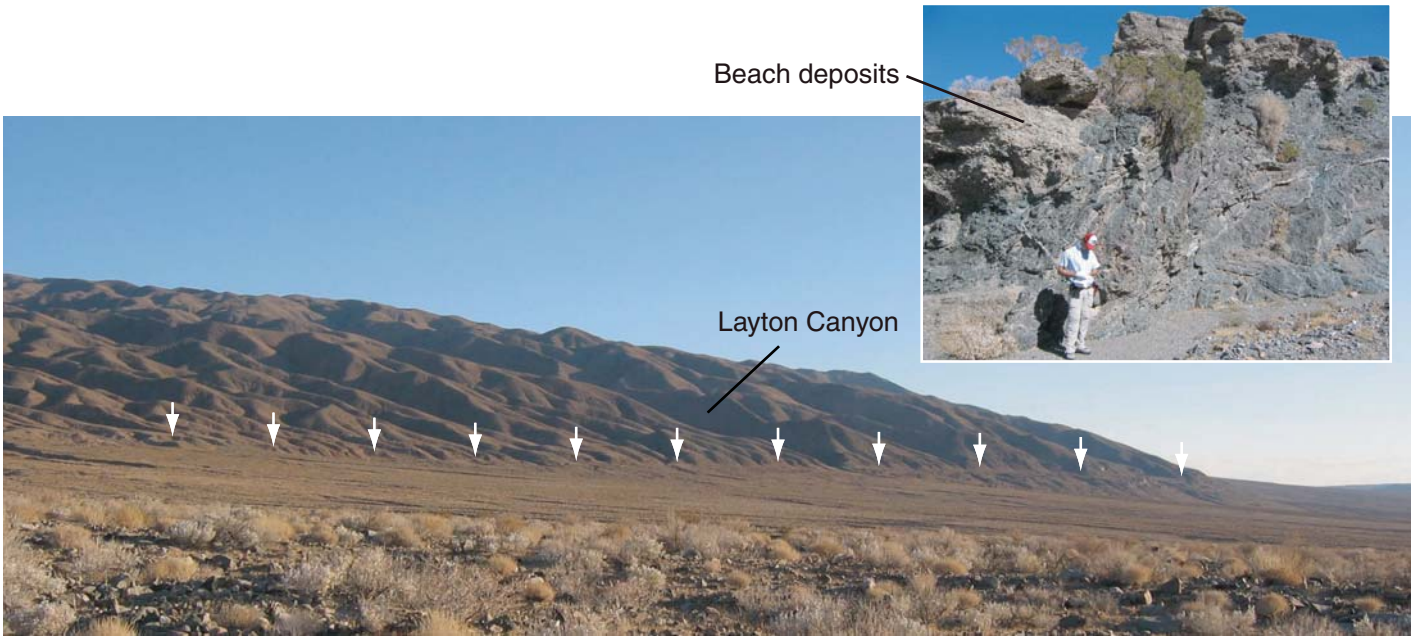

Figure 4. Photograph spanning central and southern Searles Valley. A wave-cut bench denoted by arrows marks the last highstand shoreline of Searles Lake. Inset is outcrop at head of Layton Canyon. Cemented beach deposits are perched on top of crystalline bedrock. Person for scale.

TABLE 2. RADIOCARBON AGES OF LACUSTRINE DEPOSITS IN SEARLES VALLEY

Sample ID	Lab ID[a]	Material	$\delta^{13}C$	^{14}C age[b]	Reservior corrected ^{14}C age[c]	Calendar age (2σ)[d,e]
1-1	AA61608	Buff travertine with shell fragments	+5.64	11,568 ± 68	11,239 ± 68	11,167 ± 138
2-1	AA61607	Pedogenic hardground with dense lower carbonate-cemented layer	+5.88	12,181 ± 71	11,852 ± 71	11,726 ± 187
4-1a	AA62076	Carbonate-cemented angular alluvial gravels	+5.51	13,564 ±77	13,235 ± 77	13,752 ± 394
4-1b	AA62077	Carbonate rind between rounded lacustrine cobbles	+5.38	12,564 ± 74	12,235 ± 74	12,219 ± 302
4-2	AA62078	Brown, nodular travertine	+6.26	14,485 ± 84	14,156 ± 84	14,937 ± 445

[a] Samples processed at University of Arizona Accelerator Mass Spectrometry Laboratory.
[b] Age calculated using the Libby half-life (5568 yr). Uncertainties at 1σ.
[c] Reservoir corrections performed following Lin et al. (1998).
[d] ^{14}C ages calibrated using Calib 5.0 (Stuiver and Reimer, 1993).
[e] Calibration data set: INTCAL04.14c (Reimer et al. 2004).

similarity in elevation to the highstand shoreline in southern Searles Valley recognized by McGill and Sieh (1991), we infer that this level probably represents the maximum highstand of Searles Lake. Beach gravels at Layton Canyon are cemented by thinly laminated carbonate matrix; nodular tufa occurs as 1–2 cm rinds on some clasts. Beach gravels grade basinward into debris-flow and alluvial fan units with carbonate cement surrounding clasts. Both the beach deposits and correlative alluvial fan deposits are overlain by a 1–2-m-thick, moderately sorted, clast-supported debris-flow deposit. The surface of this unit preserves only subtle bar and swale topography; clasts on the surface are moderately to well varnished and display moderately rubified undersides. This Qf2 deposit is not associated with tufa or carbonate cement, consistent with the stratigraphic observation that fan deposition postdates the last occupation of the high shoreline at Layton Canyon.

We sampled selected lacustrine tufa from key locations along the fault system for radiocarbon dating to tie our depositional interpretations to the lake-level history (Smith and Street-Perrott, 1983; Lin et al., 1998). To account for reservoir effects, we employed a correction factor following Peng et al. (1978; cf. Lin et al., 1998) (Table 2). Calibrations were performed with Calib 5.0 (Stuiver and Reimer, 1993) using the intcal04.14c calibration data set (Reimer et al., 2004). We report here the calendar year B.P. age within 2σ (Table 2). At Layton Canyon, we sampled carbonate cement (4–1a, Table 2) and massive nodular tufa (4–1b, Table 2) from alluvial gravels beneath Qf2 fans and massive nodular tufa from the sidewall of Layton Canyon (Table 2). These samples yielded ages of 14,170 ± 300 and 15,700 ± 390 cal yr B.P. In addition, one sample (4–2, Table 2) of massive, nodular tufa associated with lacustrine muds west of these samples (Fig. 2) yielded a slightly older age of 16,890 ± 450 cal yr B.P. These data suggest carbonate deposition and lacustrine conditions between 14 and 17 ka, consistent with the revised chronology of Lin et al. (1998). Our results thus suggest that beach gravels at the mouth of Layton Canyon were likely deposited during the most recent occupation of the wave-cut bench during the late Pleistocene highstand of Searles Lake (Smith and Street-Perrott, 1983). The Qf2 alluvial fan deposits that overlie these units must postdate abandonment of the shoreline after ca. 14 ka.

We collected two additional samples from lacustrine deposits along the range front. At New York Canyon, a tufa sample yielded an age of 13,120 ± 140 cal yr B.P., slightly younger than ages at Layton Canyon. South of Copper Queen Canyon (Fig. 2), a carbonate sample yielded a similar age of 13,680 ± 190 cal yr B.P. (Table 2). These samples were both collected below the ~690 m shoreline, and the ages likely reflect deposition during a recessional stage of Searles Lake. Along this part of the range front, younger fans (Qf3 and Qf4o-Qf4y) crosscut all shoreline deposits (Fig. 5); we infer that these fans most likely postdate complete desiccation of Searles Lake ca. 10 ka (Smith and Street-Perrott, 1983).

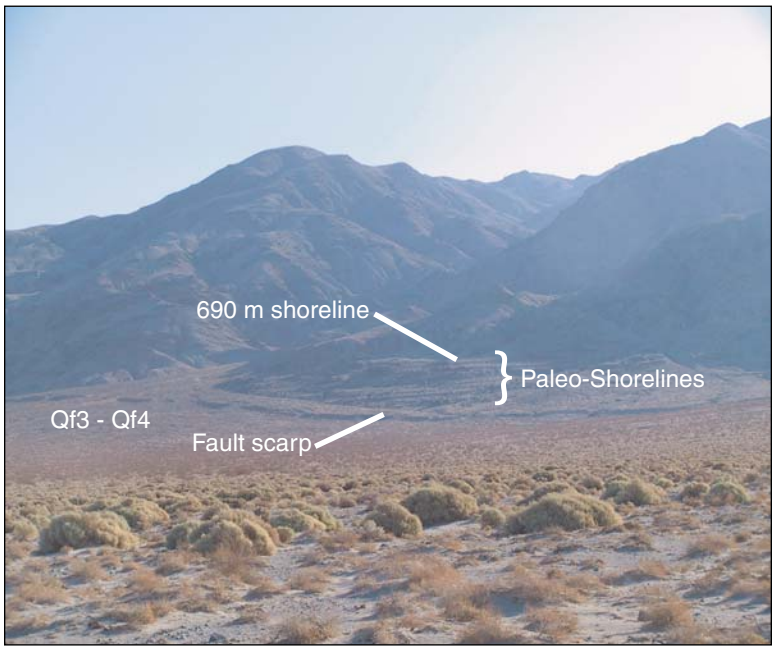

Figure 5. Looking east toward mouth of Tank Canyon. Expansive Qf3-Qf4 fans bury older lacustrine shorelines and partially obscures fault scarps at the range front.

RECENT FAULTING ALONG THE SLATE RANGE

A network of relatively fresh fault scarps developed in late Pleistocene and Holocene alluvial deposits extends from Copper Queen Canyon in the north to near the southern tip of the Slate Range, ~15 km of strike length (Fig. 2).

For simplicity of discussion, we subdivide the fault system into three sections: the southern segment extends from the southern tip of the range to Layton Canyon (Fig. 2); the central segment extends from Layton Canyon to New York Canyon; and the northern section extends from New York Canyon to Copper Queen Canyon. We mapped fault scarps and alluvial deposits along each segment. Mapping focused on two aspects of the fault system. First, we conducted high-precision topographic surveys of scarp height and utilized alluvial fan surfaces as markers of displacement. By combining these estimates of fault slip (Fig. 6) with radiocarbon dating of the displaced fan surfaces, we place bounds on slip rates averaged over late Pleistocene time. Second, we conducted detailed mapping of outcrops exposed near the intersection of the Searles Valley fault and the active range-front scarps to explore the hypothesis that these two systems are linked.

Southern Segment

A nearly continuous set of fault scarps strikes 050°–065° between the southern edge of the map area and a canyon 1 km south of Layton Canyon that we have informally named South canyon (Fig. 2). The trace of the fault is slightly sinuous along strike and appears to mimic changes in the orientation of the range front (Fig. 2). Scarp heights vary from ~0.5 to >2.5 m as they cut across at least four different alluvial fan surfaces (Fig. 2). Young Qf4o and Qf4y alluvial fans (Qf4 collectively) are offset <0.5 m along the southern map area boundary, whereas older lacustrine deposits exhibit larger displacements. We searched for indications of a component of lateral displacement, but were unable to find appropriate markers. Thus, the slip vector along this section of the fault remains uncertain. Where the range-front curves toward the north, the system changes character and the single strand splits into a zone of short discontinuous fault scarps that follow the range front (Fig. 2). Near Layton Canyon, scarps strike generally north-south and offset Qf2 alluvial surfaces between 1 and 3 m.

Central Segment

The range-front fault system strikes approximately north-south between Layton Canyon and New York Canyon, and forms a narrow graben just west of the range front (Fig. 2). Individual fault scarps vary between 1 and 5 m in height in this section and offset both Qf2 and Qf3 surfaces. At the north end of the central fault section (north of New York Canyon), the trace of the active fault terminates abruptly at a bedrock promontory in the range, nearly on strike with the southern extent of the Searles Valley fault (Fig. 2). We discuss the details of this intersection separately.

Along this section of the fault, relict alluvial surfaces provide abundant estimates of the vertical component of fault displacement. In addition, shallow channels are incised into the Qf2 surfaces, and the channel walls provide markers to assess possible oblique components of slip along the scarps. Several of the larger channels exhibit narrow (2–5 m wide) terrace deposits with well-developed boulder levees that are inset against the older fan surface (Fig. 7). Mapping and surveys of five channels along this section of the graben system reveal no discernable lateral displacements of the terrace risers or levee deposits (Fig. 7). Thus, we conclude that displacement along the central segment is primarily dip slip and records east-west extension along the western flank of the Slate Range.

Northern Segment

North of New York Canyon, the range-front fault system steps ~1 km to the west, around a bedrock salient in the range (Fig. 2). Northward from this point, the active fault trace is defined by a single, relatively continuous surface trace that strikes 345°–355°. Scarp height varies from 1.5 to 5 m and increases from south to north to a maximum near the mouth of Tank Canyon. The fault displaces all fan surfaces along this section except the modern channels. The scarp also displaces lacustrine deposits near the mouth of Sand Canyon (Fig. 2). However, the morphology of the scarp is obscured by wind-blown sand sourced from Sand Canyon, and we were unable to confidently estimate the magnitude of displacement at this point. From examining the base map (Fig. 2), it is apparent that transects 14, 15, and 16 farther north do not capture extension recorded on secondary downdip scarps. The bar and swale surface morphology of the deposits offset by these secondary scarps prevented us from being able to confidently determine what was a scarp and what was noise derived from the topography. Given the 0.5–1 m height of many of the bars, we acknowledge that the results for these three transects may underestimate the magnitude of slip along the northern segment of the fault zone.

Evidence for Pleistocene Slip on a Low-Angle Normal Fault

Geologic mapping at the northern end of the central segment reveals geometric relationships between high-angle fault scarps developed in late Pleistocene alluvium and the low-angle Searles Valley fault (Fig. 8). The Searles Valley fault is exposed within the bedrock of the Slate Range (Fig. 9, inset) from New York Canyon northward, and is marked by a west-dipping (~20°) gouge zone that truncates metamorphic units and fabrics in the footwall (Diderichsen, 2005). Southward, the Searles Valley fault appears to follow the range front, and the exhumed, eroded fault surface (now inactive) defines the topography along the western slope of the Slate Range (Fig. 10); Cichanski (2000) recognized this feature and discussed its similarity to turtleback fault surfaces in Death Valley. The central segment of the range-front fault system also parallels the range front as a system of grabens (Fig. 2). Whether these scarps represent a newly formed high-angle fault or whether they formed during slip on the low-angle detachment depends critically on the intersection between the fault systems.

Exposures of alluvial deposits in direct fault contact with bedrock occur in several gullies extending west from the range front around New York Canyon and expose the geometry of the intersection. The contact between alluvial deposits and bedrock dips shallowly west (~18º–22°) and is characterized by a 5–20-cm-thick layer of gouge overlying a highly brecciated zone of bedrock as thick as several meters (Fig. 9, inset). The hanging wall of the fault is made up of a relatively thin (<15 m) sequence of alluvial deposits. The lowermost unit comprises 3–5 m of well-sorted, fine to coarse sand exhibiting planar bedding (0.5–2 cm). The sands are moderately indurated and cemented with carbonate matrix. This unit is overlain by a 2–3-m-thick layer of gray, well-rounded, and sorted cobbles. The sorting and rounding of these clasts suggest a high-energy depositional environment, and we interpret them as beach or nearshore facies. The uppermost unit in the section is a 1–3-m-thick layer of poorly sorted, subangular fanglomerate (Fig. 9, inset). The top surface of the fanglomerate, where preserved, exhibits a moderate degree of pavement development with highly developed desert varnish on some of the larger clasts.

Overall, the stratigraphy is consistent with that observed farther south along the range. Beach and nearshore deposits, likely developed during the last retreat of the lake, are overlain by alluvial fans. The similarity of this succession to the stratigraphy at Layton Canyon and the degraded surface morphology on top of the alluvial fan units lead us to infer that the uppermost gravels are probably equivalent in age to Qf2 (ca. 12–14 ka).

Both alluvial and lacustrine deposits are cut by high- to moderate-angle, west-dipping normal faults. The lowermost beach sands immediately

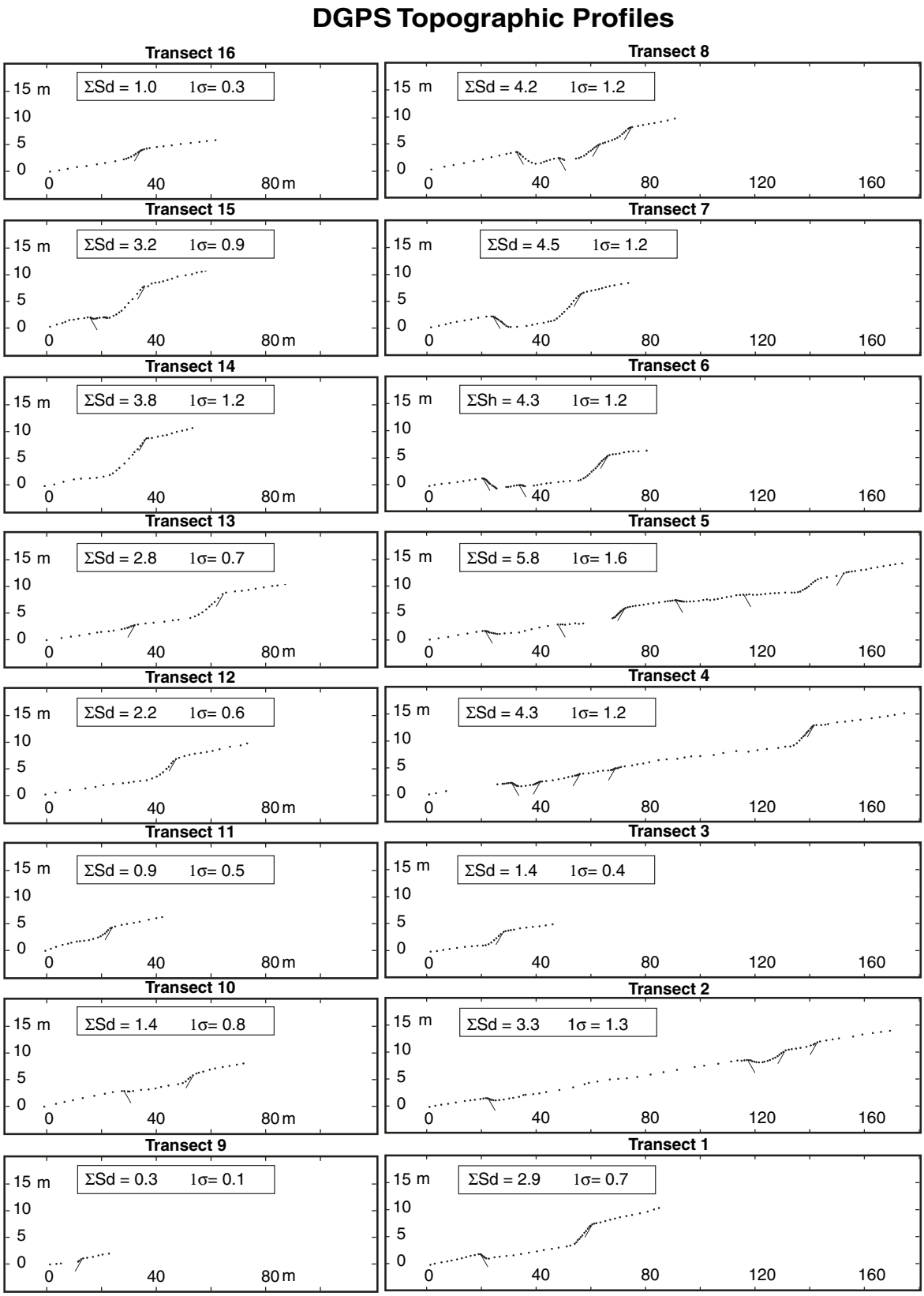

Figure 6. High-precision topographic profiles surveyed using Differential Global Positioning Satellite (DGPS). Black dots represent individual survey points. Black lines represent fault scarps. Vertical exaggeration is 1.95 for all profiles. ΣSd = cumulative slip resolved onto underlying west-dipping (20°) fault.

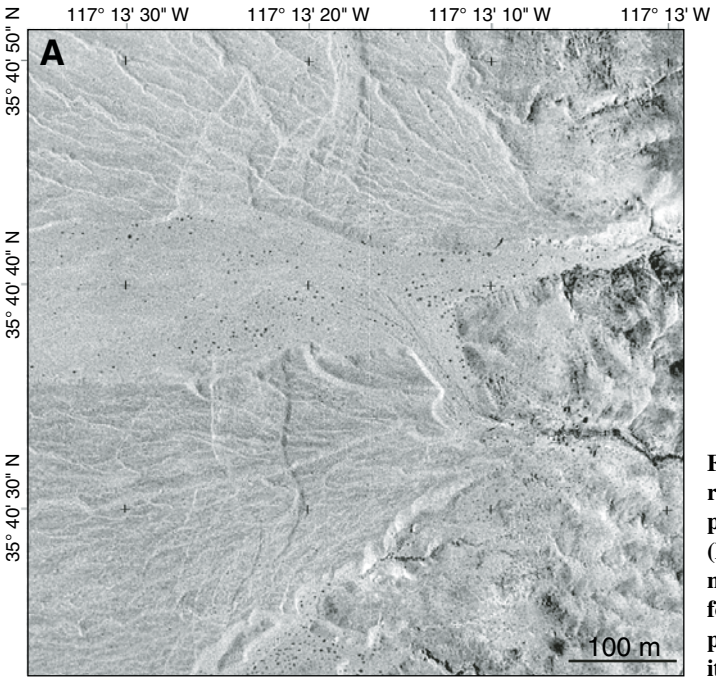

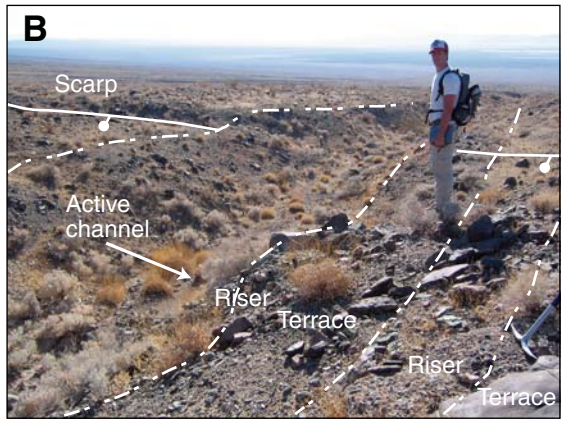

Figure 7. (A) U.S. Geological Survey digital-ortho-quarter-quadrangle (DOQQ) image of Layton Canyon. Channels are not displaced laterally, indicating that local displacement vector is dip slip. (B) Absence of lateral offset across the graben of the incised channel. Debris-flow channel deposits are inset against the main channel, forming two riser-terrace pairs. The upper riser can be used as a piercing point to measure the slip vector across the graben, because it is not prone to erosion by the active channel below.

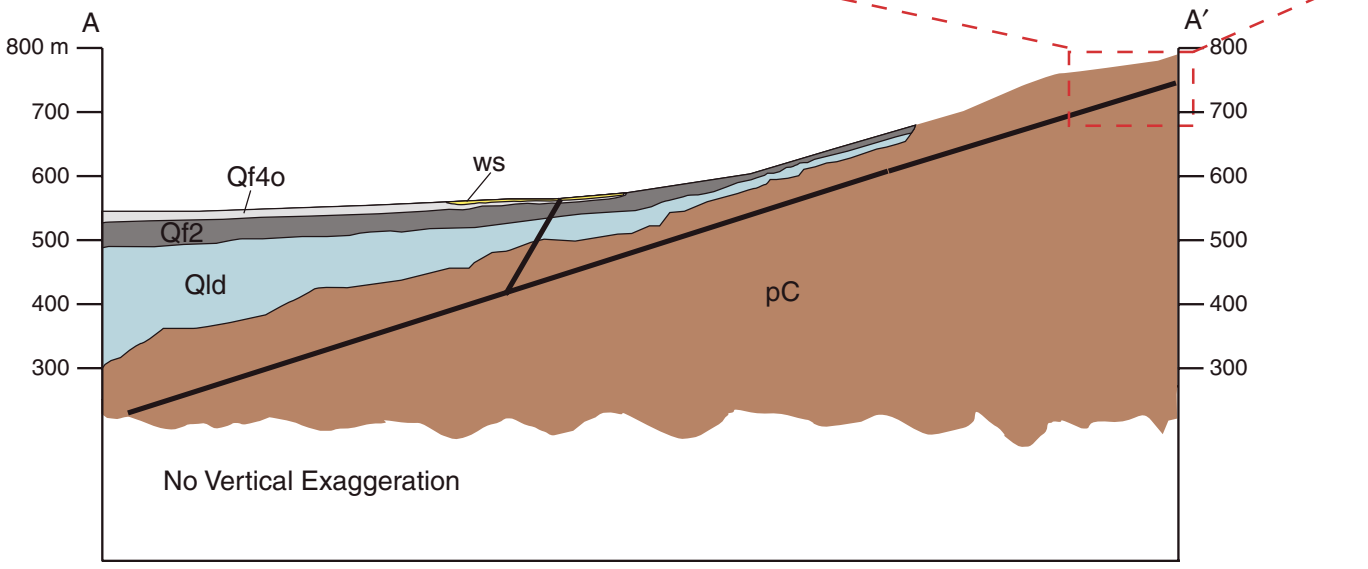

Figure 8. Cross-section A–A′ depicts the structural style of the northern segment of the Searles Valley fault. The rooted detachment (originally mapped as the Sand Canyon thrust by Smith et al., 1968) visible in the inset photograph is inferred to be intersected down dip by a steeply dipping splay fault that offsets alluvial deposits at the surface. At this location, the surface scarp associated with the splay is partially obscured by wind-blown sand derived from Sand Canyon. Relief on hillside is approximately 100 m.

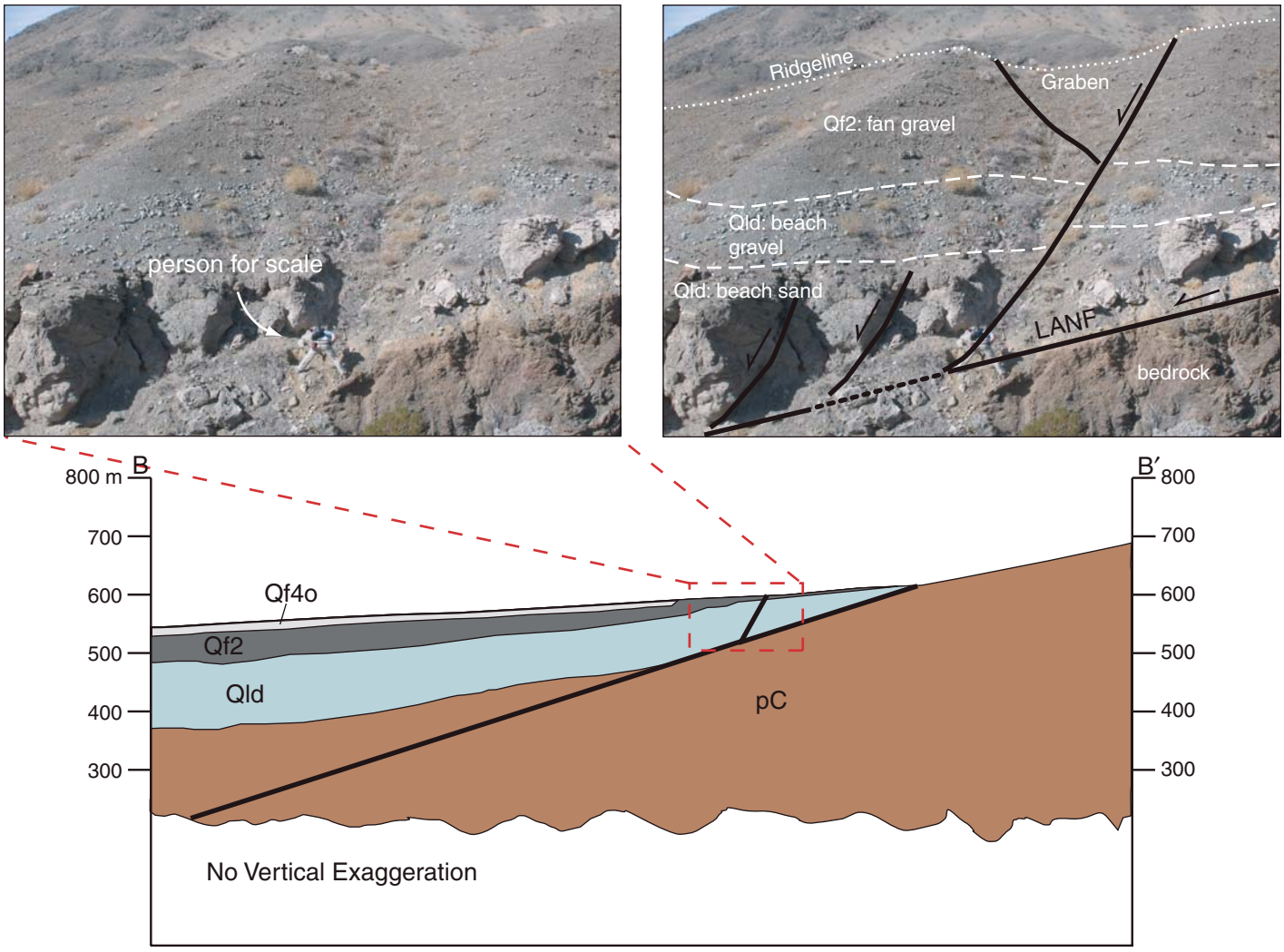

Figure 9. Cross-section B–B′ depicts structural style of the central segment of the Searles Valley fault. Photograph pairs along the eastern part of B–B′ document the relationship between young fault scarps and an underlying low-angle fault evidenced here by the 0.5–1-m-thick gouge zone. Left photograph is uninterpreted; right photograph shows our structural analysis. The low-angle fault juxtaposes Quaternary gravels and sands on top of brecciated metamorphic footwall rocks. Qf2 gravels offset at the ridgeline postdate 14 ka lacustrine deposits in Layton Canyon to the south. The steeply dipping normal fault within the Quaternary section projects downward and merges with the low-angle fault, indicating that the two structures are kinematically linked. Small splay faults propagate upward from the low-angle fault and break up cemented beach sands; these faults do not produce any measurable surface offset, and may predate deposition of overlying gravels.

above the gouge zone of the low-angle fault expose numerous normal faults with small displacements (<2–3 m) that serve to extend the section in an east-west direction (Fig. 9, inset). In addition, two large normal faults displace the entire section and form a graben (Fig. 9). These faults are expressed as scarps in the fan surface with ~1–2 m of throw. The west-dipping fault projects downward with a dip of ~60° (Fig. 9, inset). The fault, however, does not displace the low-angle gouge zone at the base of the section, but rather soles into the shallowly dipping contact (Fig. 9, inset). This relationship indicates that slip on the graben-bounding faults must have been accommodated by displacement on the low-angle detachment.

RECONSTRUCTION OF FAULT SLIP

To quantify slip since the late Pleistocene, we use relict alluvial fan surfaces as markers to reconstruct the displacement across each scarp. We conducted high-resolution topographic surveys using a survey-grade differential global positioning system (subcentimeter precision) at 16 locations along the range front (Figs. 2 and 7). Our profiles are oriented perpendicular to fault strike and parallel to extension direction. We combine topographic information with field observations of the unmodified extent of the relict surface in the hanging wall and footwall to define the gradient of the original unfaulted surface, and we fit the data using a least-squares regression (Fig. 10A). We assume that scarps are generated by a 60° dipping fault located at the midpoint of the scarp. This geometry is consistent with observations of fault dip where exposed in channel walls. Footwall and hanging-wall fan surfaces were projected laterally to their intersection with the dipping scarp segment to yield estimates of total fault slip (Table 3).

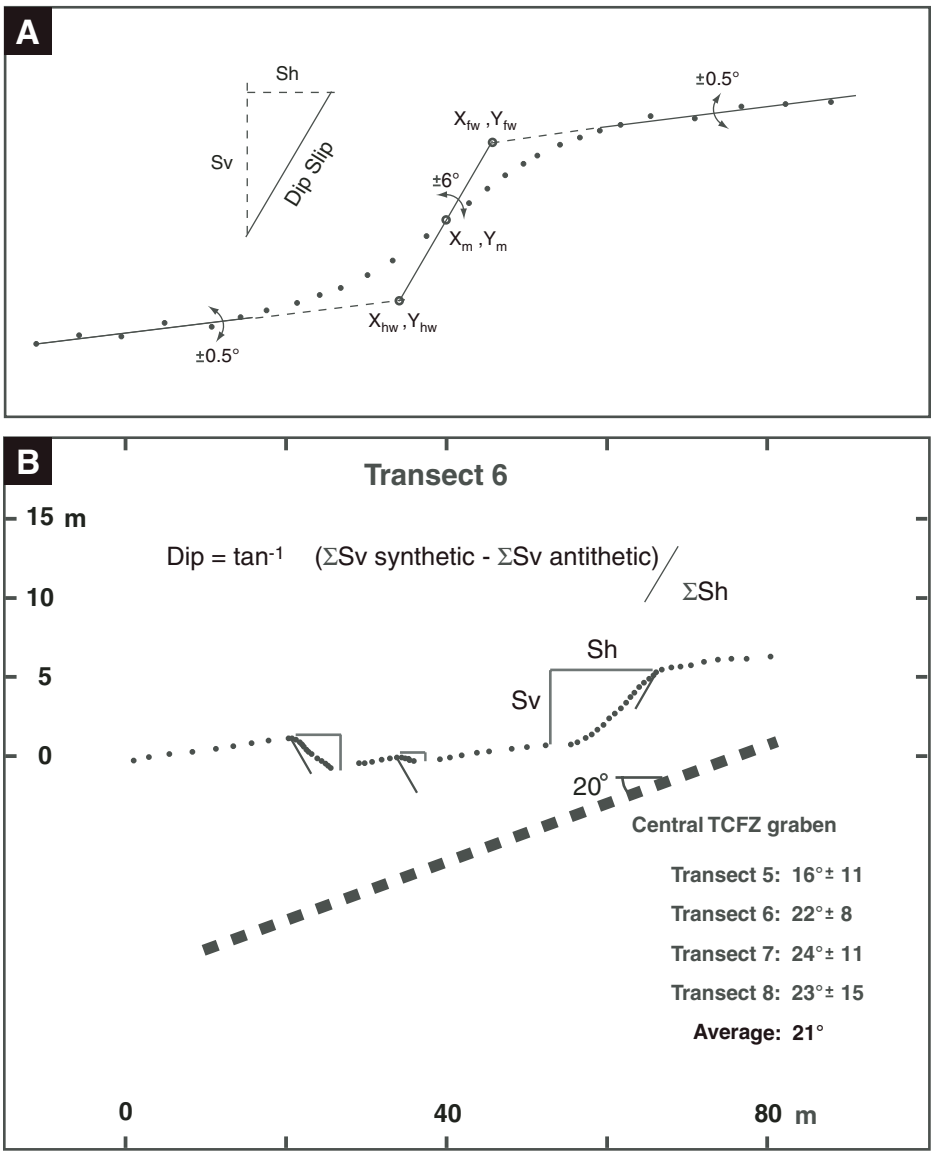

Figure 10. (A) Raw topographic profile from transect 11 (solid dots) as well as the model scarp geometry (solid and dashed lines) we used to calculate horizontal (Sh) and vertical (Sv) slip components. Solid dots are individual survey points. Solid lines on the hanging wall and footwall are least square regressions of surface slope. Dashed lines represent projected trace of the hanging walls and footwalls prior to erosion of scarp. From these data we calculated heave and throw across each scarp, by fixing the midpoint of the scarp (X_m, Y_m), and performing Monte Carlo analyses to locate the footwall (X_{fw}, Y_{fw}) and hanging wall (X_{hw}, Y_{hw}) cutoffs. (B) Simplified cross section through graben in central Searles Valley fault zone. Slip on the low-angle normal fault translates to offset on the scarp-forming faults composing the graben. The sum of the Sh and Sv components of offset across each scarp according to the supplied expression equates to the heave and throw on the underlying low-angle fault. TCFZ—Tank Canyon fault zone.

In order to estimate uncertainty in fault displacement, we performed Monte Carlo simulations that incorporate uncertainties in both the gradient of the fan surface and fault dip (Thompson et al., 2002). Uncertainties in the gradient of the fan surface were derived from individual regressions (typically, ±0.5° at 1σ), while fault dip was considered to be 60° ± 6° (1σ) (Fig. 10A). Where the fault zone consists of multiple scarps, we sum displacements on all scarps and propagate uncertainties accordingly.

Our results bear on three aspects of faulting in Searles Valley: (1) the geometry of the detachment beneath the central and southern sections of the fault system, (2) the geometry of the northern network of active faults, and (3) slip rates on the fault system as a whole. Each of these is considered separately in the following.

Bounds on Detachment Dip from Surface Displacement

Measurement of fault displacements across the central portion of the range-front graben between New York and Layton Canyons (Fig. 2) allows us to delimit the geometry of the detachment in the shallow subsurface and to test the hypothesis that slip on the graben-bounding faults is accommodated by displacement on the detachment. Following Axen et al. (1999), the ratio of cumulative throw to cumulative heave across the graben-bounding faults is a function of detachment dip. Reconstructed topographic profiles (Fig. 10B) at four locations across the graben system indicate that the fault system has relatively low throw to heave ratios. These surveys were all conducted across a fan surface of uniform age (Qf2), and thus the results are representative of the total slip since the late Pleistocene. Our results are consistent with a detachment dip between 16° and 24° (Fig. 11). Propagation of uncertainties suggests that, although each individual determination allows dips between 5° and 35° (Fig. 11), the means cluster tightly around 21° ± 2° (1σ). We note that this result is remarkably similar to dips measured along the Searles Valley fault to the north (Fig. 2), suggesting that the method adequately resolves the geometry of the detachment at depth. In addition, two profiles along the southern section of the fault system yield relatively low dips (~35°–40°), suggesting that the detachment likely changes geometry, but is continuous around the bend near Layton Canyon (Fig. 2). This analysis lends further support to the argument that displacement of young alluvium is

TABLE 3. FAULT DISPLACEMENTS

Transect	S_h (m)	S_v (m)	S_d (m)
1	2.73 ± 0.66	1.12 ± 0.29	1.12 ± 0.29
2	3.05 ± 1.20	5.19 ± 1.86	3.26 ± 1.29
3	1.33 ± 0.39	2.26 ± 0.32	1.42 ± 0.42
4	4.05 ± 1.15	5.19 ± 1.67	4.33 ± 1.24
5	5.46 ± 1.53	9.31 ± 2.36	5.84 ± 1.64
6	4.02 ± 1.15	6.87 ± 0.38	4.30 ± 1.24
7	4.24 ± 1.11	7.22 ± 1.29	4.53 ± 1.20
8	3.87 ± 1.08	6.66 ± 1.54	4.18 ± 1.17
9	0.27 ± 0.12	0.46 ± 0.17	0.29 ± 0.13
10	1.34 ± 0.70	2.28 ± 1.07	1.43 ± 0.75
11	0.82 ± 0.43	1.39 ± 0.62	0.88 ± 0.46
12	2.02 ± 0.60	3.43 ± 0.50	2.16 ± 0.64
13	2.66 ± 0.69	4.51 ± 0.55	2.84 ± 0.74
14	3.50 ± 1.07	5.97 ± 1.20	3.75 ± 1.15
15	3.01 ± 0.85	5.14 ± 0.84	3.21 ± 0.92
16	0.94 ± 0.27	1.59 ± 0.21	1.00 ± 0.29

Note: S_h is horizontal displacement; S_v is vertical displacement; S_d is displacement resolved onto low-angle fault. Detachment dip assumed equal to 20° ± 5°. Uncertainties are reported to 1σ.

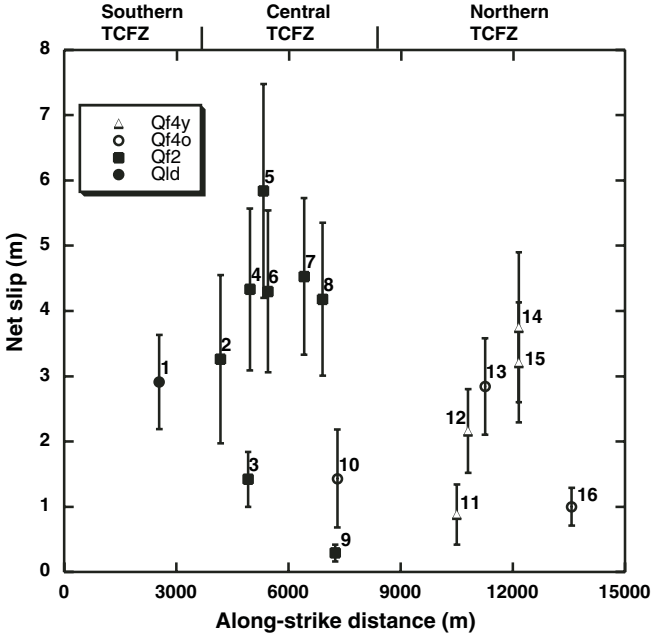

Figure 11. Net slip resolved onto 20° detachment fault (Searles Valley fault) plotted as function of distance along strike from southern map area boundary. The northern, central, and southern sections of the Searles Valley fault zone are labeled for spatial reference. Cumulative slip is shown by symbols, error bars are 1σ. Note that large uncertainties are associated with multiscarp transects. These uncertainties are the consequence of allowing the parameters outlined in Figure 10A to vary independently for each scarp. TCFZ—Tank Canyon fault zone.

accommodated on a low-angle detachment fault rooted beneath the valley, at least along the central and perhaps along the southern segments of the fault zone.

Along-Strike Variations in Fault Geometry

Although both direct observation and indirect measures of surface displacement demonstrate that high-angle faults cutting Pleistocene alluvium are kinematically linked to slip on the low-angle Searles Valley fault, the geometry of the northern section of the active fault system remains less certain. The graben projects northward to where the Searles Valley fault continues within the Slate Range (Fig. 2). At this point, the trace of the recent scarps steps ~1 km westward (Fig. 2) and curves around a bedrock promontory near Sand Canyon. Northward from this point, the fault scarp trends subparallel with the trace of the Searles Valley fault for ~3 km before terminating near Copper Queen Canyon.

Along the northern segment, seven transects yielded estimates of net slip between ~0.8–3.7 m (Fig. 6). Displacement estimates tend to be greatest near the center of the fault segment and decrease toward the tips (Fig. 6). The pattern is similar to displacement gradients on normal faults observed globally (e.g., Dawers et al., 1993; Cowie and Roberts, 2001) and suggests that this section of the fault probably represents an individual segment. Unlike the distributed faulting evidenced by the graben along the central segment, the northern segment is generally characterized by a single, west-facing fault scarp. Thus, we are unable to directly assess whether this fault is linked to the Searles Valley detachment at depth. However, given that the active trace of this fault appears to terminate northward along the range front, and given the apparent connection between the Searles Valley fault and a low-angle fault system near the crest of the range at Manly Pass (Fig. 2, inset) (Walker et al., 2005), we find it likely that the northern scarps simply represent a hanging-wall splay above the primary Searles Valley fault (Fig. 8).

Slip Rates over the Late Pleistocene

Our results place bounds on the average slip rates along both the central and northern sections of the range-front fault system. Given direct and indirect evidence for a shallowly dipping detachment beneath Searles Valley, we model total fault slip across the central graben by resolving the net horizontal extension observed at the surface onto a plane dipping ~15º–20°. We propagate uncertainties in fault slip using a Monte Carlo approach (mean dip of 20° ± 5º). On the northern segment, we take a conservative approach and simply infer that all slip occurs on a high-angle (~60°) fault. A single survey across the southern segment of the fault zone yields a displacement estimate of ~3 m, but is not discussed further due to the paucity of data.

Six transects surveyed across Qf2 surfaces along the central segment record a mean net fault slip of 4.4 ± 0.8 m when resolved onto the underlying detachment (Fig. 11). We exclude from this mean value data from younger surfaces (Qf4o-Qf4y) because they likely average displacement over a shorter time interval (e.g., transect 10). In addition, two transects from the Qf2 surfaces yielded relatively low values; we suspect that these result from incomplete preservation of scarps adjacent to active alluvial fans (transect 9, Fig. 2) and incomplete survey coverage (transect 3). Excluding these points, the resultant displacement yields an average slip rate of 0.21–0.35 m/k.y. over the past ~15–17 k.y. Any slip between bedrock and alluvial deposits where the Searles Valley fault surfaces at the range front will add to this estimate. Relations at this contact unfortunately do not allow us to make any assessment, and possible contributions are ignored in the discussion in the following.

Displacement on the northern part of the fault system appears to increase from south to north (Fig. 11), consistent with a steep displacement gradient near the tip of the fault segment. Displacement decreases rapidly toward Copper

Queen Canyon, consistent with the absence of scarps farther north along the range front. Thus, our surveys suggest that the northern segment has a mean displacement of 2.3 ± 0.6 m. Alluvial fans along this segment of the fault are almost all younger (Qf4 deposits; Fig. 2) than fans along the central section, and preclude a direct comparison with the magnitude of slip across the central segment. Nonetheless, if we presume that Qf4o-Qf4y surfaces are both younger than 10 ka, slip rates averaged over this time are thus ~0.17–0.29 m/k.y., similar to rates inferred from Qf2 surfaces. Faulting within the range would add to this estimate, but it is not assessed at present.

Given the relatively young age of alluvial deposits in Searles Valley, our rate estimates could be somewhat biased by seismic cycle effects, particularly if the recurrence interval of rupture events is long. Unfortunately, we have only one site at which faults displace surfaces of varying age (Fig. 11). Here, displacement is ~4 m in surfaces of Qf2 age, but only ~2 m in Qf4 surfaces. This suggests that slip along the Searles Valley fault system accumulated during multiple moderate earthquakes. We note that this is consistent with global scaling relationships (Wells and Coppersmith, 1994) that suggest that typical surface displacements are ~1 m for an ~20-km-long normal fault. However, we have no data with which to address the possibility of clustered seismicity (Rockwell et al., 2000) or longer-term variations in slip rate.

DISCUSSION AND IMPLICATIONS

Our results suggest a complicated geometry of active faults along the margin of Searles Valley and within the Slate Range. Displacement of late Pleistocene alluvium along the southern and central section of the active range-front fault appears to be linked to slip on a low-angle (~20°) detachment. These sections of the fault system are marked by regionally extensive graben systems (Fig. 8). In contrast, although the geometry of the northern section is less certain, displacement of Holocene fans occurs along a single west-facing series of scarps, consistent with slip on a high-angle normal fault. We suspect that these differences in the expression of active faults are not coincidental, but rather reflect the mechanics of hanging-wall deformation. In particular, distributed deformation and the formation of graben is a likely consequence of a deformation in a relatively thin (<100 m) layer of weakly cohesive alluvial sediments above the detachment. Axen et al. (1999) observed similarly distributed faulting above a low-angle detachment in Baja California. The northern section of the range-front fault system, however, reaches the surface ~1.5 km west of where Searles Valley fault is exposed in the range (Fig. 2). Simple geometric considerations suggest that these two faults must intersect ~200 m beneath the surface. Thus, we interpret the northern section of the range-front fault system as a high-angle, hanging-wall splay of the Searles Valley fault system. We cannot prove, but believe it likely, that it too merges with the detachment at depth (Fig. 8).

These variations in fault geometry have important implications for the strain transfer between the Searles Valley and Panamint Valley fault systems. Late Pleistocene slip rates appear to be similar on the central and northern sections of the range-front fault system in Searles Valley. However, the fact that recent displacement on the range-front fault system does not extend north of Copper Queen Canyon (Fig. 2) requires slip to either die out along the range front or be accommodated within the bedrock of the range. We suggest, following Walker et al. (2005), that active deformation must be accommodated along the detachment within the Slate Range. The Searles Valley fault continues northward within the range, beyond Copper Queen Canyon, and joins the Manly Pass fault near the crest of the range (Diderickson, 2005). This fault is also a west-dipping low-angle fault that carries Miocene volcanics and Pliocene gravels in its hanging wall, indicating that it has been active in the latter part of the Tertiary. We argue that our results require that the Searles Valley fault remained active as a low-angle structure into late Pleistocene time, and that they suggest that the Manly Pass fault may also have undergone recent slip.

Our results suggest that slip rates over the late Pleistocene and Holocene are significantly slower (~0.2–0.4 mm/yr) than inferred in previous studies (~1 mm/yr, Wesnousky, 1986). Fault slip results in net extension in an east-west direction, such that the detachment plays only a minor role in the present-day budget of transcurrent shear. It is intriguing that such a low-angle structure has remained active in a regime that favors the development of strike-slip and/or transtensional faults (e.g., Unruh et al., 2003). This appears to require a relatively weak fault (e.g., Wesnousky and Jones, 1994), perhaps consistent with recent determinations of mechanical properties of fault gouge from the Panamint Valley fault system (Numelin et al., 2007).

Our observations and analysis of late Pleistocene and recent faulting in Searles Valley represent one of only a handful of studies to demonstrate active slip on a low-angle normal fault (Hayman et al., 2003; Abbott et al., 2001; Axen et al., 1999; Caskey et al., 1996). Our field observations at the northern end of the graben leave little doubt that scarp-forming displacement in the shallow subsurface is accommodated by slip on a low-angle detachment. This conclusion is similar to that reached by Hayman et al. (2003) from outcrop observations of slip on the Black Mountain detachment, and an extensional critical wedge model (e.g., Xiao et al., 1991). Although the age of the youngest displaced hanging-wall sediments (0.18–0.1 Ma) represent a longer time period than this study, both studies suggest that a component of active deformation in the southwestern Basin and Range is accommodated by low-angle faults in the shallow crust.

ACKNOWLEDGMENTS

This research was partially supported by the Tectonics program at the National Science Foundation (EAR-0409169 - EK), by grants from Sigma Xi, the Geological Society of America, and the American Association of Petroleum Geologists (TJN), and by the Geology Associates Fund at the University of Kansas (BD). Frank Monastero at the Geothermal Energy Division of the Department of the Navy was instrumental in facilitating access to the field site and providing logistical support. We thank Joe Andrew for help in the field and Kurt Frankel and Mike Oskin for reviews that significantly improved the clarity of the manuscript.

REFERENCES CITED

Abbott, R.E., Louie, J.N., Caskey, S.J., and Pullammanappallil, S., 2001, Geophysical confirmation of low-angle normal slip on the historically active Dixie Valley fault, Nevada: Journal of Geophysical Research, v. 106, p. 4169–4181, doi: 10.1029/2000JB900385.

Abers, G.A., Mutter, C.Z., and Fang, J., 1997, Shallow dips of normal faults during rapid extension: Earthquakes in the Woodlark-D'Entrecasteaux rift system, Papua New Guinea: Journal of Geophysical Research, v. 102, no. B7, p. 15,301–15,317, doi: 10.1029/97JB00787.

Atwater, T., and Stock, J.M., 1998, Pacific Northwest America plate tectonics of the Neogene southwestern United States—An update: International Geology Review, v. 40, p. 375–402.

Axen, G.J., 2004, Mechanics of low-angle normal faults, *in* Karner, G., Taylor, B., Driscoll, N., and Kohlstedt, D.L., eds., Rheology and Deformation in the Lithosphere at Continental Margins: Columbia University Press, p. 46–91.

Axen, G.J., Fletcher, J.M., Cowgill, E., Murphy, M., Kapp, P., MacMillan, I., Ramos-Velazquez, E., and Aranda-Gomez, J., 1999, Range-front fault scarps of the Sierra El Mayor, Baja California: Formed above an active low-angle normal fault?: Geology, v. 27, p. 247–250, doi: 10.1130/0091-7613(1999)027<0247:RFFSOT>2.3.CO;2.

Beanland, S., and Clark, M.M., 1994, The Owens Valley fault zone, eastern California, and surface faulting associated with the 1872 earthquake: U.S. Geological Survey Bulletin, v. 1982, p. 29.

Bennett, R.A., Wernicke, B.P., Niemi, N.A., Friedrich, A.M., and Davis, J.L., 2003, Contemporary strain fields in the

northern Basin and Range province from GPS data: Tectonics, v. 22, p. 1008, doi: 10.1029/2001TC001355.

Boncio, P., Brozzetti, F., and Lavecchia, G., 2000, Architecture and seismotectonics of a regional low-angle normal fault zone in central Italy: Tectonics, v. 19, p. 1038–1055, doi: 10.1029/2000TC900023.

Burchfiel, B.C., and Stewart, J.H., 1966, 'Pull-apart' origin of the central segment of Death Valley, California: Geological Society of America Bulletin, v. 77, p. 439–441, doi: 10.1130/0016-7606(1966)77[439:POOTCS]2.0.CO;2.

Burchfiel, B.C., Hodges, K.V., and Royden, L.H., 1987, Geology of Panamint Valley–Saline Valley pull-apart system, California: Palinspastic evidence for low-angle geometry of a Neogene range-bounding fault: Journal of Geophysical Research, v. 92, p. 10,422–10,426.

Caskey, S.J., Wesnousky, S.G., Zhang, P., and Slemmons, D.B., 1996, Surface faulting of the 1954 Fairview Peak (M_S 7.2) and Dixie Valley (M_S 6.8) earthquakes, central Nevada: Seismological Society of America Bulletin, v. 86, p. 761–787.

Cichanski, M., 2000, Low-angle, range-flank faults in the Panamint, Inyo, and Slate ranges, California: Implications for recent tectonics of the Death Valley region: Geological Society of America Bulletin, v. 112, p. 871–883, doi: 10.1130/0016-7606(2000)112<0871:LARFFI>2.3.CO;2.

Cowie, P.A., and Roberts, G.P., 2001, Constraining slip rates and spacings for active normal faults: Journal of Structural Geology, v. 23, p. 1901–1915, doi: 10.1016/S0191-8141(01)00036-0.

Dawers, N.H., Anders, M.H., and Scholz, C.H., 1993, Growth of normal faults: Displacement-length scaling: Geology, v. 21, p. 1107–1110, doi: 10.1130/0091-7613(1993)021<1107:GONFDL>2.3.CO;2.

Didericksen, B., 2005, Middle Miocene to recent faulting and exhumation of the central Slate Range, Eastern California Shear Zone [M.S. thesis]: Lawrence, University of Kansas, 104 p.

Dixon, T.H., Robaudo, S., Lee, J., and Reheis, M.C., 1995, Constraints on present-day Basin and Range deformation from space geodesy: Tectonics, v. 14, p. 755–772, doi: 10.1029/95TC00931.

Dixon, T.H., Miller, M., Farina, F.H., and Johnson, D., 2000, Present-day motion of the Sierra Nevada block and some tectonic implications for the Basin and Range province, North American Cordillera: Tectonics, v. 19, p. 1–24.

Dixon, T.H., Norabuena, E., and Hotaling, L., 2003, Paleoseismology and global positioning system: Earthquake-cycle effects and geodetic versus geologic fault slip rates in the Eastern California shear zone: Geology, v. 31, p. 55–58, doi: 10.1130/0091-7613(2003)031<0055:PAGPSE>2.0.CO;2.

Dokka, R.K., and Travis, C.J., 1990, Role of the Eastern California Shear Zone in accommodating Pacific–North American plate motion: Geophysical Research Letters, v. 17, p. 1323–1326.

Friedrich, A.M., Lee, J., Wernicke, B.P., and Sieh, K., 2004, Geologic context of geodetic data across a Basin and Range normal fault, Crescent Valley, Nevada: Tectonics, v. 23, p. TC2015, doi: 10.1029/2003TC001528.

Gan, W., Svarc, J.L., Savage, J.C., and Prescott, W.H., 2000, Strain accumulation across the eastern California shear zone at latitude 36°30′N: Journal of Geophysical Research, v. 105, p. 16,229–16,236, doi: 10.1029/2000JB900105.

Hayman, N.W., Knott, J.R., Cowan, D.S., Nemser, E., and Sarna-Wojcicki, A.M., 2003, Quaternary low-angle slip on detachment faults in Death Valley, California: Geology, v. 31, p. 343–346, doi: 10.1130/0091-7613(2003)031<0343:QLASOD>2.0.CO;2.

Jackson, J.A., and White, N.J., 1989, Normal faulting in the upper continental crust: Observations from regions of active extension: Journal of Structural Geology, v. 11, p. 15–36, doi: 10.1016/0191-8141(89)90033-3.

Jannik, N.O., Phillips, F.M., Smith, G.I., and Elmore, D., 1991, A ^{36}Cl chronology of lacustrine sedimentation in the Pleistocene Owens River system: Geological Society of America Bulletin, v. 103, p. 1146–1159, doi: 10.1130/0016-7606(1991)103<1146:ACCOLS>2.3.CO;2.

Kirby, E., Snyder, N., Whipple, K., Walker, J.D., and Andrew, J., 2003, Neotectonics of the Panamint Valley fault zone: Active slip on a low-angle normal fault system: Eos (Transactions, American Geophysical Union), fall meeting supplement, v. 84, no. 46, abstract T51D-0194.

Lavier, L.L., and Buck, W.R., 2002, Half graben versus large-offset low-angle normal fault: Importance of keeping cool during normal faulting: Journal of Geophysical Research, v. 107, 2122, doi:10.1029/2001JB000513.

Lin, J.C., Broecker, W.S., Hemming, S.R., Hajdas, I., Anderson, R.F., Smith, G.I., Kelley, M., and Bonani, G., 1998, A reassessment of U-Th and C-14 ages for late-glacial high-frequency hydrological events at Searles Lake, California: Quaternary Research, v. 49, p. 11–23, doi: 10.1006/qres.1997.1949.

Longwell, C.R., 1945, Low angle normal faults in the Basin and Range province: American Geophysical Union Transactions, v. 26, p. 107–118.

McGill, S.F., and Sieh, K., 1991, Surficial offsets on the central and eastern Garlock fault associated with prehistoric earthquakes: Journal of Geophysical Research, v. 96, p. 21,597–21,621.

McQuarrie, N., and Wernicke, B.P., 2005, An animated tectonic reconstruction of southwest North America since 36 Ma: Geosphere, v. 1, p. 147–172, doi: 10.1130/GES00016.1.

Miller, M.G., 1999, Implications of ductile strain on the Badwater turtleback for pre-14 Ma extension in the Death Valley region, California, *in* Wright, L.A., and Troxel, B.W., eds., Cenozoic basins of the Death Valley region: Geological Society of America Special Paper 333, p. 115–126.

Miller, M.M., Johnson, D.J., Dixon, T.H., and Dokka, R., 2001, Refined kinematics of the Eastern California shear zone from GPS observations, 1993–1998: Journal of Geophysical Research, v. 106, p. 2245–2263, doi: 10.1029/2000JB900328.

MIT, and Biehler, S., 1987, A geophysical investigation of the Northern Panamint Valley, Inyo County, California: Evidence for possible low-angle normal faulting at shallow depth in the crust: Journal of Geophysical Research, v. 92, p. 10,427–10,441.

Niemi, N., Wernicke, B.P., Brady, R.J., Saleeby, J.B., and Dunne, G.C., 2001, Distribution and provenance of the middle Miocene Eagle Mountain Formation, and implications for regional kinematic analysis of the Basin and Range province: Geological Society of America Bulletin, v. 113, p. 419–442, doi: 10.1130/0016-7606(2001)113<0419:DAPOTM>2.0.CO;2.

Numelin, T., Marone, C., and Kirby E., 2007 Frictional properties of natural fault gouge from a low-angle normal fault, Panamint Valley, California: Tectonics, v. 26, TC2004, doi:10.1029/2005TC001916.

Park, S.K., and Wernicke, B., 2003, Electrical conductivity images of Quaternary faults and Tertiary detachments in the California Basin and Range: Tectonics, v. 22, p. 1030, doi: 10.1029/2001TC001324.

Peltzer, G., Crampe, F., Hensley, S., and Rosen, P., 2001, Transient strain accumulation and fault interaction in the Eastern California shear zone: Geology, v. 29, p. 975–978, doi: 10.1130/0091-7613(2001)029<0975:TSAAFI>2.0.CO;2.

Peng, T.H., Goddard, J.G., and Broecker, W.S., 1978, A direct comparison of ^{14}C and ^{230} Th ages at Searles Lake, California: Quaternary Research, v. 9, p. 319–329, doi: 10.1016/0033-5894(78)90036-4.

Reheis, C., and Sawyer, T.L., 1997, Late Cenozoic history and slip rates of the Fish Lake Valley, Emigrant Peak, and Deep Springs fault zones, Nevada and California: Geological Society of America Bulletin, v. 109, p. 280–299, doi: 10.1130/0016-7606(1997)109<0280:LCHASR>2.3.CO;2.

Reimer, P.J., and 27 others, 2004, INTCAL04.14c calibration dataset: Radiocarbon, v. 10, p. 1029–1058.

Rockwell, T.K., Lindvall, S., Herzberg, M., Murbach, D., Dawson, T., and Berger, G., 2000, Paleoseismology of the Johnson Valley, Kickapoo, and Homestead Valley faults: Clustering of earthquakes in the Eastern California Shear Zone: Seismological Society of America Bulletin, v. 90, p. 1200–1236, doi: 10.1785/0119990023.

Smith, G.I., and Street-Perrott, F.A., 1983, Pluvial lakes of the western United States, *in* Porter, S.C., ed., The late Pleistocene (late Quaternary environments of the United States): Minneapolis, University of Minnesota Press, p. 190–212.

Smith, G.I., Troxel, B.W., Gray, C.H.J., and Von Huene, R., 1968, Geologic reconnaissance of the Slate Range, San Bernardino and Inyo counties, California: San Francisco, California Division of Mines and Geology, 33 p.

Snow, J.K., and Wernicke, B.P., 2000, Cenozoic tectonism in the central basin and range: Magnitude, rate, and distribution of upper crustal strain: American Journal of Science, v. 300, p. 659–719, doi: 10.2475/ajs.300.9.659.

Stuiver, M., and Reimer, P., 1993, Calib version 5.0: Radiocarbon, v. 35, p. 215–230.

Thompson, S.C., Weldon, R.J., Rubin, C.M., Abdrakhmatov, K., Molnar, P., and Berger, G.W., 2002, Late Quaternary slip rates across the central Tien Shan, Kyrgyzstan, central Asia: Journal of Geophysical Research, v. 107, 2203, doi:10.1029/2001JB000596.

Unruh, J., Humphrey, J., and Barron, A., 2003, Transtensional model for the Sierra Nevada frontal fault system, eastern California: Geology, v. 31, p. 327–330, doi: 10.1130/0091-7613(2003)031<0327:TMFTSN>2.0.CO;2.

Walker, J.D., Kirby, E., and Andrew, J.E., 2005, Strain transfer and partitioning between the Panamint Valley, Searles Valley, and Ash Hill fault zones, California: Geosphere, v. 1, p. 111–118, doi: 10.1130/GES00014.1.

Wells, D.L., and Coppersmith, K.J., 1994, New empirical relationships among magnitude, rupture length, rupture width, rupture area, and surface displacement: Seismological Society of America Bulletin, v. 84, p. 974–1002.

Wernicke, B., 1995, Low-angle normal faults and seismicity: A review: Journal of Geophysical Research, v. 100, p. 20,159–20,174, doi: 10.1029/95JB01911.

Wernicke, B., and Snow, J.K., 1998, Cenozoic tectonism in the central Basin and Range: Motion of the Sierran–Great Valley Block: International Geology Review, v. 40, p. 403–410.

Wesnousky, S.G., 1986, Earthquakes, Quaternary faults, and seismic hazard in California: Journal of Geophysical Research, v. 91, p. 12,587–12,631.

Wesnousky, S.G., and Jones, C.H., 1994, Oblique slip, slip partitioning, spatial and temporal changes in the regional stress field, and the relative strength of active faults in the Basin and Range, western United States: Geology, v. 22, p. 1031–1034, doi: 10.1130/0091-7613(1994)022<1031:OSSPSA>2.3.CO;2.

Xiao, H.B., Dahlen, F.A., and Suppe, J., 1991, Mechanics of extensional wedges: Journal of Geophysical Research, v. 96, p. 10,301–10,318.

Zhang, P., Ellis, M., Slemmons, D.B., and Mao, F., 1990, Right-lateral displacements and the Holocene slip rate associated with prehistoric earthquakes along the Southern Panamint Valley fault zone: Implications for Southern Basin and Range tectonics and coastal California deformation: Journal of Geophysical Research, v. 95, p. 4857–4872.

Manuscript Received 26 May 2006
Revised Manuscript Received 29 December 2006
Manuscript Accepted 7 March 2007